CELLULAR NEUROSCIENCE

IL4-driven microglia modulate stress resilience through BDNF-dependent neurogenesis

Jinqiang Zhang[1,2], Peijing Rong[3], Lijuan Zhang[1], Hui He[1], Tao Zhou[2], Yonghua Fan[1], Li Mo[1], Qiuying Zhao[1], Yue Han[1], Shaoyuan Li[3], Yifei Wang[3], Wan Yan[1], Huafu Chen[1]*, Zili You[1]*

Adult neurogenesis in the dentate gyrus of the hippocampus is regulated by specific microglia groups and functionally implicated in behavioral responses to stress. However, the role of microglia in hippocampal neurogenesis and stress resilience remains unclear. We identified interleukin 4 (IL4)–driven microglia characterized by high expression of Arg1, which is critical in maintaining hippocampal neurogenesis and stress resistance. Decreasing Arg1+ microglia in the hippocampus by knocking down the microglial IL4R suppressed hippocampal neurogenesis and enhanced stress vulnerability. Increasing Arg1+ microglia in the hippocampus by enhancing IL4 signaling restored hippocampal neurogenesis and the resilience to stress-induced depression. Brain-derived neurotrophic factor (BDNF) was found necessary for the proneurogenesis effects of IL4-driven microglia. Together, our findings suggest that IL4-driven microglia in the hippocampus trigger BDNF-dependent neurogenesis responding to chronic stress, helping protect against depressive-like symptoms. These findings identify the modulation of a specific microglial phenotype as a treatment strategy for mood disorders.

INTRODUCTION

It is well known that prolonged stress can induce cascading effects in the inflammatory system and lead to neuropsychiatric disorders, such as depression and anxiety, which can affect neurogenesis (1). New neurons are generated throughout adulthood in two regions of the brain, the dentate gyrus (DG) in the hippocampus and the subventricular zone (2). Neural stem/progenitor cells (NSPCs) undergo proliferation, differentiation, survival, and maturation into new neurons, which eventually integrate into the neural network (3). These processes are regulated negatively by stressful experiences and positively by treatment with antidepressant drugs through altering the neurogenic microenvironment (2). These adult-born neurons are critical for mood control and behavioral output (2, 4). Alterations in the magnitude of this continuous production of new neurons are associated with both the pathophysiology of depression and the efficacy of antidepressants (5).

Microglia, the principal immune cells in the brain, play central roles in immune surveillance and maintenance of brain homeostasis (6). Studies have shown that microglia can regulate neurogenesis by secreting various factors that modulate the neurogenic microenvironment (7, 8). Under stress or pathological conditions, microglia secrete inflammatory mediators that disrupt neuronal function and impair neurogenesis, increasing the vulnerability to stress and promoting the occurrence and development of depression (7, 9). On the other hand, recent evidence showed that microglial "alternative activation" leads to an increase in adult neurogenesis in response to exercise and environmental enrichment, which contribute to normal behavior (10, 11). The role of microglia in neurogenesis depends on the balance between the soluble factors released by microglial cells under different activation scenarios. Microglial brain-derived neurotrophic factor (BDNF) is an important mediator of microglia-to-neuron communication and contributes to many facets of brain function via its high-affinity receptor, tropomyosin-related kinase B (TrkB) (12, 13). Microglial BDNF may also be involved in neurobehavioral plasticity and neurogenesis and therefore may underlie the pathophysiology of depression (14, 15).

Interleukin 4 (IL4) is a multifunctional cytokine expressed in the brain and is involved in the regulation of inflammatory responses and physiological processes of the central nervous system (CNS) (16, 17). IL4 deficiency weakens the resilience against stress-induced depression, while increasing IL4 levels can alleviate depressive-like behaviors (18, 19). Studies have shown that IL4 can reprogram microglia toward an Arg1+ phenotype for maintaining brain homeostasis, neuroprotection, and tissue repair (20, 21). However, the effects of IL4-induced Arg1+ microglia on neurogenesis and stress resilience are poorly understood.

In light of the role of microglia in the pathogenesis of depressive disorders, we hypothesized that promoting a neuroprotective phenotype of microglia would improve stress responses and depressive behaviors. Consistent with this expectation, we found that in mice exposed to chronic mild stress (CMS), overexpression of hippocampal IL4 drove Arg1+ microglia to promote neurogenesis, which, in turn, attenuated depressive-like behaviors.

RESULTS

Vulnerability to stress is associated with reduced IL4 signaling in the hippocampus

Following exposure to CMS for 3 weeks, C57BL/6J mice were separated into high-susceptible (HS) and low-susceptible (LS) subpopulations according to their sucrose preference and immobility time in tail suspension test (TST) and forced swim test (FST) (Fig. 1A). We examined cytokines, chemokines, and neurotrophic factors related to neuroinflammatory processes in the hippocampus and prefrontal cortex and found that levels of IL4 mRNA in the hippocampus were elevated in LS mice but reduced in HS mice, compared to the control mice (Fig. 1B). In particular, the change in IL4 protein levels in the hippocampus was the most significant outcome

[1]School of Life Science and Technology, University of Electronic Science and Technology of China, Chengdu 610054, China. [2]Guizhou University of Traditional Chinese Medicine, Guiyang 550025, China. [3]Institute of Acupuncture and Moxibustion, China Academy of Chinese Medical Sciences, Beijing, China.
*Corresponding author. Email: youzili@uestc.edu.cn (Z.Y.); chenhf@uestc.edu.cn (H.C.)
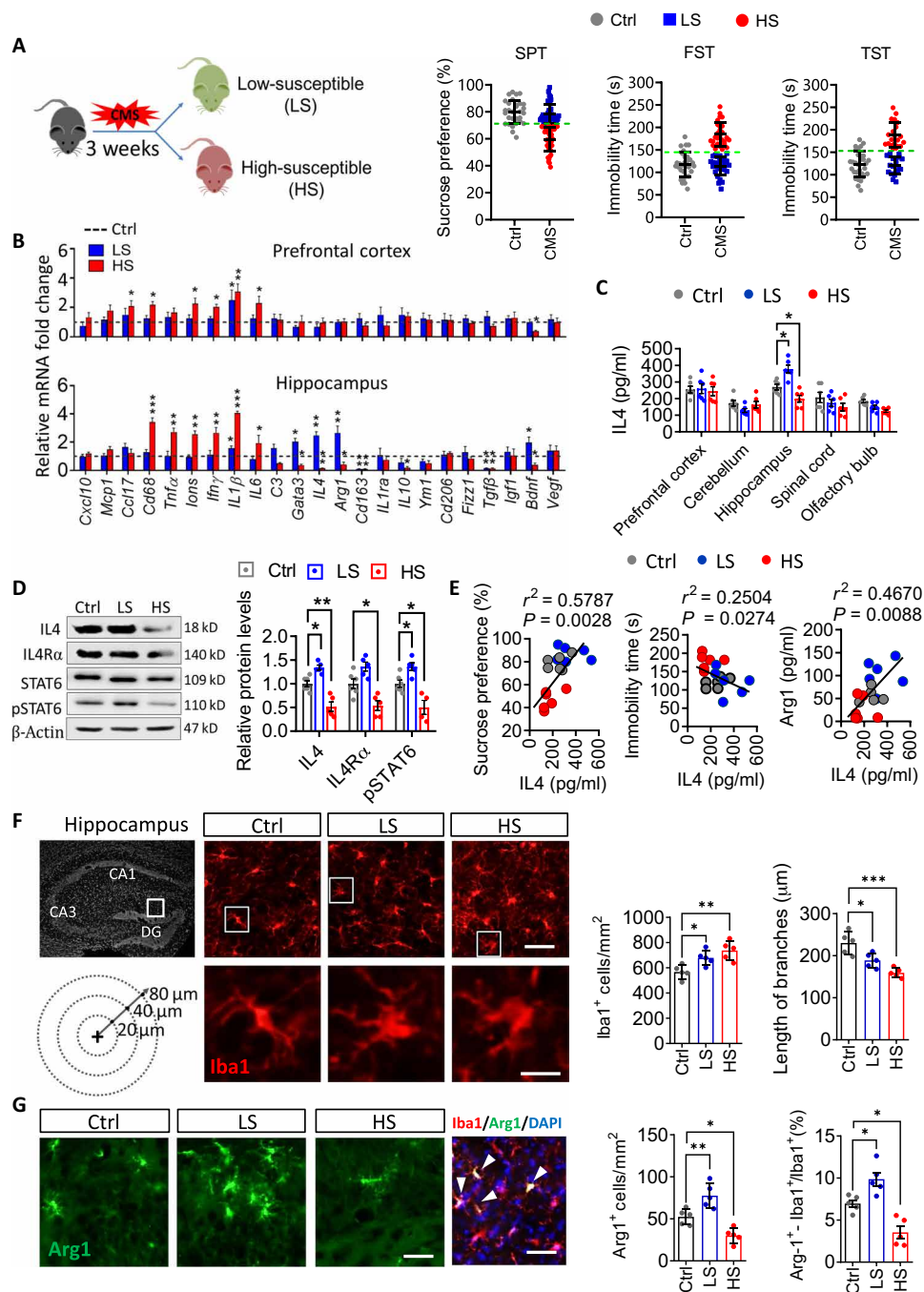
Fig. 1. Hippocampal IL4 levels and Arg1+ microglia are involved in resistance of mice to stress. (**A**) Behavioral screening of LS and HS subpopulations of mice exposed to 3-week CMS. (**B**) Quantitative PCR to examine mRNA expression of cytokines, chemokines, growth factors, and trophic factors in the hippocampus and prefrontal cortex of HS and LS mice. Data are standardized to control group (n = 4 to 6, each sample in triplicate). (**C**) Enzyme-linked immunosorbent assay to assay the protein level of IL4 in prefrontal cortex, cerebellum, hippocampus, amygdala, and olfactory bulb of control, HS, and LS mice. Each circle represents one mouse (n = 6, each sample in triplicate). (**D**) Western blotting shows the levels of IL4, IL4 receptor α chain (IL4Rα), STAT6, and pSTAT6 in the hippocampus of control, HS, and LS mice. IL4 and IL4Rα are normalized to β-actin, and the pSTAT6 is normalized to STAT6. (n = 4 to 6, each sample in triplicate). (**E**) Correlation between sucrose preference or immobility duration in TST, hippocampal Arg1 levels, and hippocampal IL4 levels in CMS-exposed mice. Each circle represents one mouse (n = 6). (**F**) Morphological characters of hippocampal microglia in control, HS, and LS mice. Scale bars, 50 μm (top) and 10 μm (bottom). The histogram represents the quantification of number and branch length of Iba1+ cells in hippocampus. Each dot in the bar graph represents the average of all micrograph (five to six micrographs for each mouse) in each mouse (n = 5). (**G**) Immunofluorescence micrographs and quantification of Arg1+ microglia in hippocampus of control, LS, and HS mice (n = 5). Scale bars, 50 μm. Data are presented as means ± SEM. *P < 0.05, **P < 0.01, ***P < 0.005, one-way ANOVA with Tukey test (B, C, D, F, and G). DAPI, 4′,6-diamidino-2-phenylindole.

(Fig. 1C and fig. S1). The results from in situ RNA analysis of the hippocampus with RNAscope approach showed that IL4 mRNA was expressed in neurons and microglia, more abundant in mature neurons of LS mice (fig. S1). Western blotting showed that hippocampal IL4–signal transducers and activators of transcription 6 (STAT6) signaling was increased in LS mice but decreased in HS mice (Fig. 1D). Correlation analysis showed that the IL4 concentration in the hippocampus positively correlated with sucrose preference and negatively correlated with immobility time in TST (Fig. 1E), suggesting that the vulnerability of mice to CMS was associated with reduced IL4 signaling in the hippocampus.

Considering the pivotal roles of microglia in neuroinflammatory processes, we examined microglial morphology and characteristics. The hippocampal microglia showed significant activation morphology (increased number, expanded cell body, and shortened branches) after CMS exposure, especially in HS mice (Fig. 1F). Notably, Arg1^{+} microglia, a class of microglial phenotype with neuroprotective functions, was found to increase in hippocampus of LS mice, but decrease in hippocampus of HS mice (Fig. 1G).

Overexpression of IL4 in the hippocampus induced microglial Arg1^{+} phenotype

Since IL4 is a rapidly degraded glycoprotein of about 20 kDa that cannot cross the blood-brain barrier (16), we specifically increased IL4 levels in the hippocampus using recombinant adeno-associated virus (rAAV) vectors combined with Ef1α promoter encoding murine IL4 to investigate the effect of brain-derived IL4 on Arg1^{+} microglia and stress resistance (Fig. 2A). Overexpression of IL4 in the hippocampus was confirmed by immunofluorescence assay, with higher abundances of IL4 being located in NeuN^{+} cells (fig. S2A). IL4 receptor α chain (IL4Rα), STAT6, and pSTAT6 were examined with Western blotting at 2 weeks after injection of the recombinant systems (fig. S2B). Transcriptome sequencing was performed to explore the whole transcriptome levels of the hippocampus during AAV-IL4 and/or CMS treatment by RNA sequencing (RNA-seq) (fig. S3). There were 65 genes differentially expressed in AAV + CMS mice when compared to AAV mice (31 showed up-regulation and 34 down-regulation). Most of these genes are involved in stress responses. There were 760 genes with differential expression in AAV-IL4 + CMS mice compared to AAV + CMS mice (597 showed up-regulation and 163 down-regulation). Most of these genes are involved in immunomodulation (Fig. 2B and fig. S3C). Several of the genes were confirmed to be significantly and differentially expressed in the hippocampus by quantitative polymerase chain reaction (PCR). Among them, Arg1 was the most significantly up-regulated both at the gene and protein levels after AAV-IL4 injection with or without CMS treatment. In contrast, IL4 overexpression inhibited the increase of inducible nitric oxide synthase (iNOS) (an Arg1-antagonistic enzyme, promoting the production of nitric oxide) in CMS-exposed mice (Fig. 2, C and D).

To determine the cell source of Arg1, we performed cell localization of Arg1. Immunohistochemical staining showed that Arg1 was located in hippocampal Iba1^{+} cells, and the number of Arg1^{+} microglia was significantly elevated in hippocampus of AAV-IL4 mice under both nonstress and stress conditions. Microglia in the hippocampus of AAV-IL4 mice showed obvious morphological changes, manifested by decreased processes and larger somata (Fig. 2E). To assay the population of microglial subsets, flow cytometry was performed on single-cell suspensions of the whole hippocampus. The

results revealed that microglia, in the form of CD45^{int}-CD11b^{+} cells, increased significantly in CMS-exposed mice and AAV-IL4 mice, corroborating the presence of microglia proliferation. The CD86^{+}-CD206^{+} microglia were significantly increased in the hippocampus of AAV-IL4 mice (Fig. 2F).

Knockdown of microglial IL4Rα decreased Arg1^{+} microglia phenotype in the hippocampus

We observed that the microglial IL4 receptor signal was attenuated in hippocampus of HS mice but enhanced in LS mice (Fig. 3A). To confirm the effects of IL4 on microglial phenotype, knockdown of the microglial IL4 receptor was performed. The lentivirus encoding IL4Rα-targeting short hairpin RNA (shRNA) (LV-U6-LoxP-CMV-EGFP-LoxP-IL4Rα-shRNA, LoxP-shIL4Rα) was first synthesized. The transfection efficiency of LoxP-shIL4Rα on microglia and the efficiency of Cre recombinant enzyme were then confirmed in the hippocampus of CX₃CR1[Cre/ERT2] mice (fig. S4). The lentivirus vector with LoxP-shIL4Rα was injected in hippocampus of CX₃CR1[Cre/ERT2] mice, and then the mice were treated with tamoxifen for a week. We found that the microglial IL4Rα, STAT6, pSTAT6, and Arg1 were significantly reduced in the hippocampus (Fig. 3B). We thus achieved IL4Rα shRNA-specific targeting to hippocampal microglia (shIL4Rα/M).

The subliminal CMS (sCMS) paradigm was adopted to assess the correlation of Arg1^{+} microglia and stress vulnerability. Even when exposed to sCMS, shIL4Rα/M mice showed significant depressive-like behaviors, decreased Arg1^{+} microglia, and worsened neuroinflammatory responses (Fig. 3C). Knockdown of microglial IL4Rα also decreased the number of Arg1^{+} microglia in the hippocampus of AAV or AAV-IL4 mice, under both nonstress and stress conditions. Knockdown of microglial IL4Rα suppressed the proliferation of microglia and the decrease in length of branches in the hippocampus of AAV or AAV-IL4 CX₃CR1[Cre/ERT2] mice, under nonstress and stress conditions (Fig. 3D).

IL4-driven Arg1^{+} microglia enhanced hippocampal neurogenesis in CMS-exposed mice

We observed that the adult hippocampal neurogenesis was attenuated in HS mice not in LS mice (Fig. 4A). Gene ontology (GO) enrichment analysis of differentially expressed genes (DEGs) in transcriptome sequencing showed that CMS affected expression of genes associated with stress response, apoptosis, and synaptic function. Overexpression of IL4 in the hippocampus of CMS-exposed mice resulted in changes related to neurogenesis, such as the nutrient metabolism, Notch, and Wnt pathways (Fig. 4B).

We examined hippocampal neurogenesis, including proliferation, differentiation, survival, and maturity of NSPCs in CMS- and/or AAV-IL4–treated mice. The results showed that CMS-exposed mice displayed a notable reduction in neuronal differentiation, as shown by a lower number of 5-bromo-2′-deoxyuridine–positive (BrdU[+])– (DCX^{+}) cells. Overexpression of IL4 with AAV expression system in the hippocampus reversed CMS-induced deficits in neurogenesis (fig. S5A). Meanwhile, knockdown of microglial IL4Rα decreased BrdU[+]-DCX[+] (Doublecortin) cells in AAV or AAV-IL4 mice (Fig. 4C).

To assay the extent of survival and maturity of proliferative cells, the proliferating cells were labeled with BrdU before CMS exposure. Reduced numbers of surviving cells (BrdU[+]) and mature neurons (BrdU[+]-NeuN[+]) were found in DG of CMS-exposed mice.
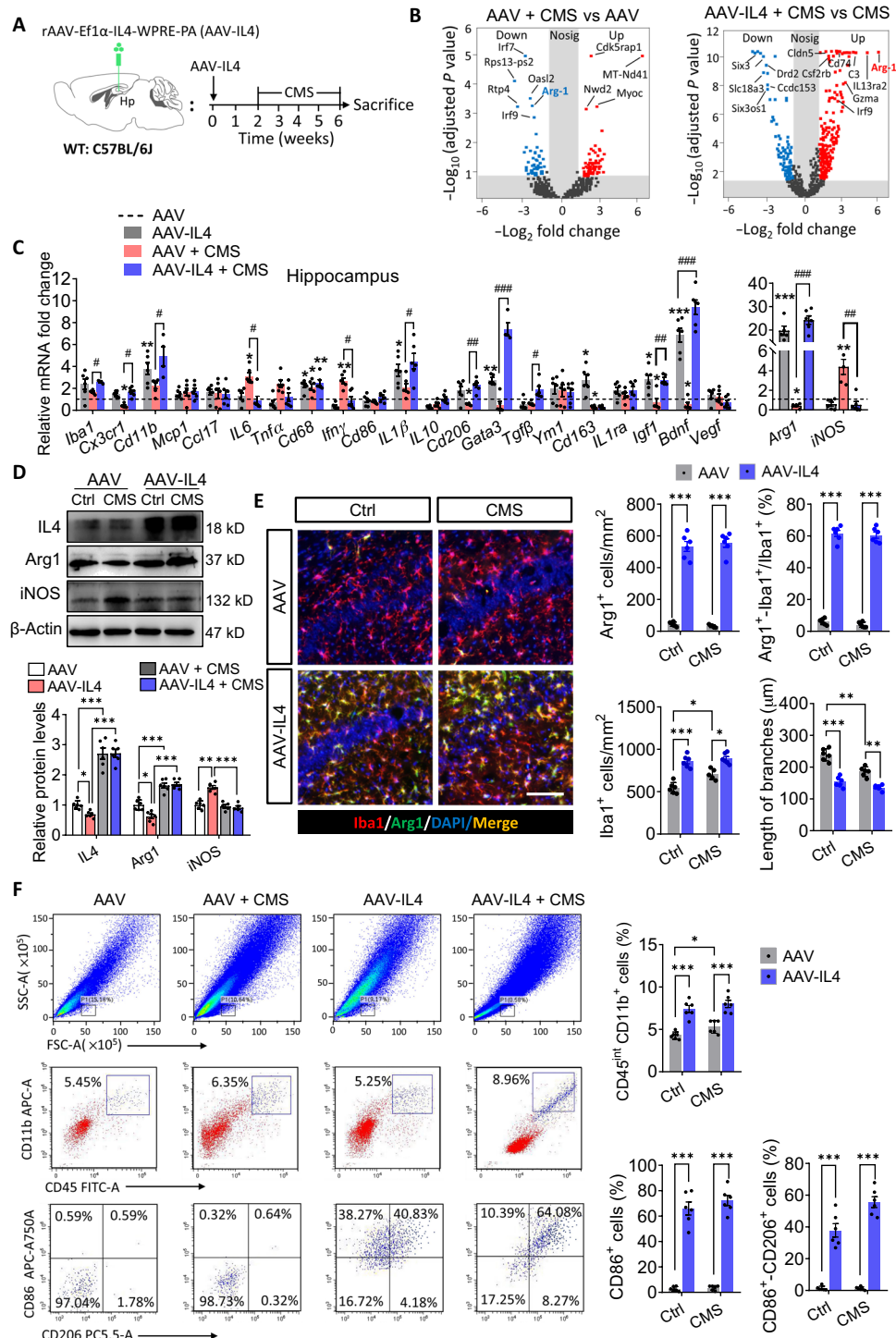
Fig. 2. Overexpression of IL4 in the hippocampus enhanced Arg1+ microglia phenotypes and mediated neuroinflammatory responses to CMS paradigm. (**A**) Experimental timeline of IL4 overexpression in the hippocampus and CMS protocol. (**B**) Volcano maps indicate differentially expressed genes (DEGs) in the brains of CMS-exposed and/or AAV-IL4–treated mice. (**C**) Quantitative PCR examination of the expression of several DEGs in the hippocampus of mice ($n = 4$ to 6). (**D**) Western blotting shows the levels of IL4, Arg1, and iNOS in the hippocampus of CMS-exposed and/or AAV-IL4–treated mice ($n = 5$ to 6). (**E**) Morphological characters of Arg1+ microglia in hippocampus. Scale bar, 100 μm. The histogram represents the quantification of number and branch length of Arg1+-Iba1+ cells in hippocampus. Each dot in the bar graph represents the average of five to six micrographs in each mouse ($n = 6$). (**F**) Flow cytometry of single-cell suspension of the whole hippocampus for microglia (CD45^{int}-CD11b+ cells), activated microglia (CD86+ cells), and anti-inflammatory microglia (CD86+-CD206+ cells). The histogram represents the quantification of CD45^{int}-CD11b+ cells, CD86+ cells, and CD86+-CD206+ cells ($n = 5$ to 6). Data are presented as means ± SEM. *$P < 0.05$, **$P < 0.01$, ***$P < 0.005$ versus AAV + Ctrl group, #$P < 0.05$, ##$P < 0.01$, ###$P < 0.005$ versus AAV + CMS group, two-way ANOVA with Tukey test (C); *$P < 0.05$, **$P < 0.01$, ***$P < 0.005$, two-way ANOVA with Tukey test (D, E, and F). FITC A, fluorescein isothiocyanate area (FITC-A).
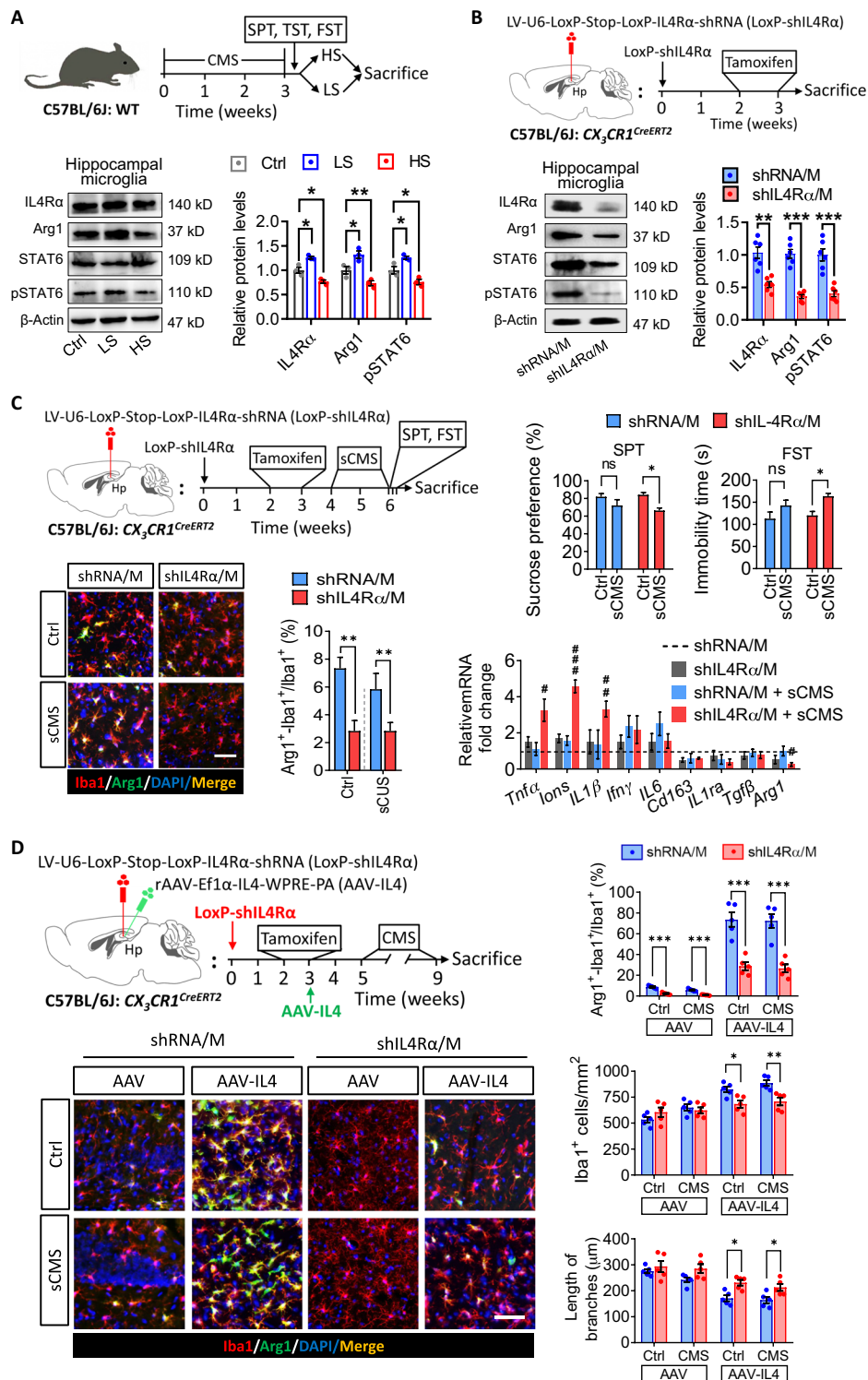
Fig. 3. Knockdown of microglial IL4Rα decreased the Arg1+ microglia phenotype in the hippocampus and increased the vulnerability of mice to stress. (**A**) Western blotting shows the levels of IL4Rα, Arg1, STAT6, and pSTAT6 in the hippocampal microglia of LS and HS mice ($n = 3$). (**B**) Western blotting shows the levels of IL4Rα, Arg1, STAT6, and pSTAT6 in the hippocampal microglia of LoxP-shIL4Rα–injected $CX_3CR1^{Cre/ERT2}$ mice after tamoxifen treatment ($n = 6$). (**C**) Effects of knockdown microglial IL4Rα combined with sCMS exposure on depressive-like behaviors, percentage of Arg1+ microglia, and cytokine expression of $CX_3CR1^{Cre/ERT2}$ mice ($n = 8$ for behavioral analysis, $n = 6$ for quantification of Arg1+ microglia, $n = 4$ to 6 for analysis of cytokine expression). Scale bar, 50 μm. (**D**) Effects of microglial IL4Rα knockdown in the hippocampus on the ratio of Arg1+ microglia, number, and length of branches of Iba1+ cells ($n = 5$). Scale bar, 50 μm. Data are presented as means ± SEM. $*P < 0.05$, $**P < 0.01$, $***P < 0.005$, one-way ANOVA with Tukey test (A), two-tailed t test (B), two-way ANOVA with Bonferroni test for behavioral analysis (C), and two-way ANOVA with Tukey test for quantification of Arg1+ microglia (C), $\#P < 0.05$, $\#\#P < 0.01$, $\#\#\#P < 0.005$ versus shRNA/M + sCMS group, two-way ANOVA with Tukey test for analysis of cytokine expression (C).
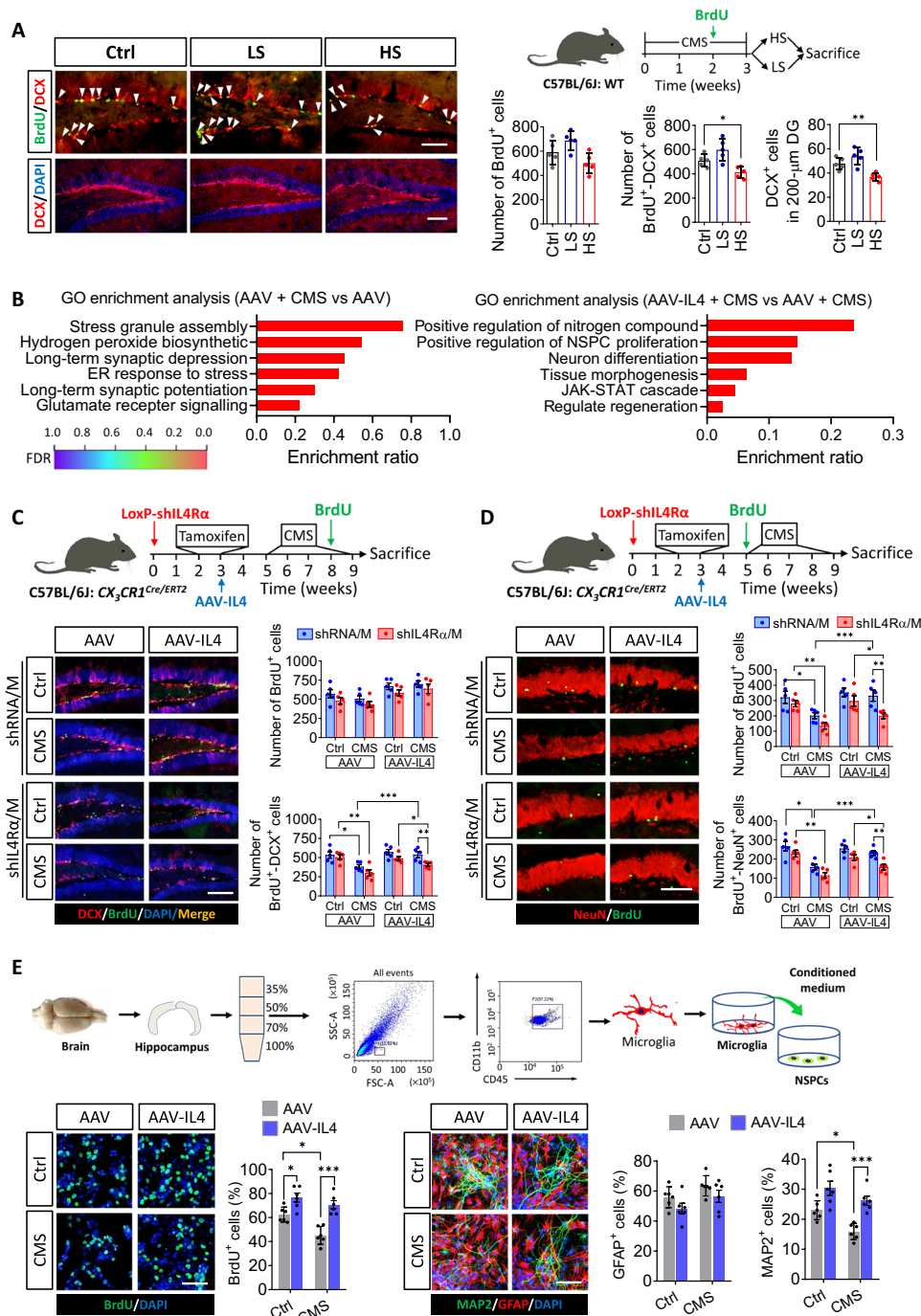
Fig. 4. IL4-driven Arg1$^+$ microglia enhanced hippocampal neurogenesis in CMS-exposed mice. (**A**) Immunofluorescence micrographs and quantification show the hippocampal neurogenesis of LS and HS mice ($n = 5$). (**B**) GO enrichment analysis for DEGs in the hippocampus of CMS-exposed mice. ER, endoplasmic reticulum; FDR, false discovery rate. (**C**) Effects of IL4 overexpression and/or microglial IL4Rα down-regulation on NSPC proliferation and differentiation in the hippocampus of *CX$_3$CR1$^{Cre/ERT2}$* mice. Representative fluorescence micrographs showing DCX expression and BrdU incorporation in the subgranular zone (SGZ). Scale bar, 100 μm. Quantification of total number of BrdU$^+$ cells, total number of DCX$^+$-BrdU$^+$ cells, and percentage of DCX$^+$-BrdU$^+$ cells out of all BrdU$^+$ cells in the neurogenic zones ($n = 5$). (**D**) Effects of IL4 over-expression and/or microglial IL4Rα down-regulation in the hippocampus (before IL4 overexpression) on NSPC survival and maturation. Representative fluorescence micrographs illustrating NeuN expression and BrdU incorporation in the SGZ. Scale bar, 100 μm. Quantification of total number of BrdU$^+$ cells, BrdU$^+$-NeuN$^+$ cells, and DCX$^+$-NeuN$^+$ cells in DG ($n = 5$). (**E**) Effects of conditioned medium from microglia isolated from hippocampus on NSPC proliferation. Proliferation was monitored by quantifying the percentage of BrdU$^+$ cells ($n = 6$). Scale bar, 50 μm. Representative micrographs of NSPCs cultured for 7 days in conditioned culture medium from microglia isolated from hippocampus. Cells were immunolabeled with glial fibrillary acidic protein (GFAP) to identify astrocytes and MAP2 to identify neurons. Percentages of GFAP$^+$ cells and MAP2$^+$ cells are quantified ($n = 6$). Scale bar, 30 μm. Data are presented as means ± SEM. *$P < 0.05$, **$P < 0.01$, ***$P < 0.005$, one-way ANOVA with Tukey test (A) and two-way ANOVA with Tukey test (C, D, and E).

Overexpression of IL4 reversed the CMS-induced decrease in the numbers of BrdU^{+} cells and BrdU[+]-NeuN^{+} cells in DG (fig. S5B). Knockdown of microglial IL4Rα decreased BrdU^{+} cells and BrdU[+]-NeuN^{+} cells in AAV or AAV-IL4 mice (Fig. 4D).

Considering that microglia can modulate neurogenesis, we collected the conditioned medium of microglia isolated from the hippocampus of AAV mice or AAV-IL4 mice under stress or nonstress conditions to culture NSPCs (Fig. 4E). Compared with the microglia-conditioned medium (M-CM) from AAV mice without CMS exposure, that from mice with CMS exposure decreased the percentage of BrdU^{+} cells, MAP2^{+} cells, and NG2^{+} cells. The opposite effects were observed with M-CM from AAV-IL4 mice without CMS. The M-CM from AAV-IL4 mice with CMS exposure increased the percentage of BrdU^{+} cells, MAP2^{+} cells, and NG2^{+} cells, when compared the M-CM from mice injected with AAV and with CMS exposure (Fig. 4E and fig. S6, A and B). Knockdown of microglial IL4Rα reversed the increase of neurogenesis in AAV-IL4 mice (fig. S6C). This suggested that CMS-induced microglia suppressed the proliferation and differentiation of NSPCs, and IL4-driven microglia promoted the proliferation and differentiation of NSPCs in the hippocampus of CMS-exposed mice. The M-CM from IL4-stimulated primary microglia had a similar effect on proliferation and differentiation of NSPCs. However, there were no significant effects on proliferation and differentiation of NSPCs after they were treated with IL4 when compared with phosphate-buffered saline (fig. S6, D to F).

IL4-driven microglia enhance neurogenesis via a BDNF-dependent pathway

Next, we explored how IL4-driven Arg1^{+} microglia may promote neurogenesis. In the transcriptome study, the expression of *Bdnf* was significantly up-regulated in the brain of AAV-IL4 + CMS mice. This suggested that IL4-driven microglia may promote hippocampal neurogenesis through BDNF signaling pathways. We confirmed that BDNF-TrkB signaling was attenuated in hippocampus of HS and AAV + CMS mice but enhanced in LS and AAV-IL4 + CMS mice (Fig. 5, A and B, and fig. S7A). The BDNF in hippocampal microglia (Iba1^{+} cells) was detected with *Bdnf*-RNAscope (Fig. 5C) and immunohistochemistry (fig. S7B). The up-regulated expression of BDNF at mRNA level was observed in hippocampal microglia of AAV-IL4–treated mice (Fig. 5D). Notably, we found that BDNF is widely distributed in both intracellular and extracellular compartments of Arg1^{+} microglia (Fig. 5E). These results suggested that IL4-driven microglia could synthesize and secrete more BDNF. Knockdown of microglial IL4Rα significantly reduced BDNF expression in the hippocampus of AAV-IL4 mice (Fig. 5F).

To determine whether BDNF was necessary and sufficient for IL4-rescued neurogenesis, AAV-IL4 mice were treated with K252a to block the TrkB pahway (fig. S7C). We found that K252a treatment blocked the increase in DCX^{+} cells and BrdU[+]-DCX^{+} cells in the hippocampus of AAV-IL4 mice subjected to the CMS paradigm (Fig. 5G). In primary culture, microglia receiving IL4 stimulation could significantly promote the expression and secretion of BDNF (Fig. 5H). Blocking of the BDNF/TrkB signaling was able to impede the increase of DCX^{+} cells when NSPCs were cultured in conditioned medium from IL4-exposed primary microglia or hippocampal microglia (Fig. 5I and fig. S7, D and E). These results suggest that BDNF is necessary for the proneurogenesis effects of IL4-driven microglia in CMS-exposed mice.

IL4-driven Arg1^{+} microglia protected mice from stress-induced depressive-like behaviors

We examined the effects of IL4 overexpression on resistance of mice to stress-induced depression using a series of behavioral tests. After 4 weeks of CMS exposure, AAV mice showed less sucrose preference, longer immobility time in FST than nonstressed control animals. As expected, these depressive-like behaviors were significantly absent in AAV-IL4 mice exposed to CMS (Fig. 6A and fig. S8, A to D). Through correlation analysis, we found that sucrose preference and immobility time in FST were positively and negatively correlated, respectively, with the percentage of Arg1^{+} microglia, BDNF concentration, and BrdU[+]-DCX^{+} cells in the hippocampus (Fig. 6B). After knockdown of microglial IL4Rα in the hippocampus, AAV-IL4 *CX₃CR1*[Cre/ERT2] mice showed depressive-like behaviors after 4-week CMS exposure (Fig. 6C and fig. S8, E to H). As mentioned above, IL4-driven microglia modulate hippocampal neurogenesis in a BDNF-dependent manner in CMS-treated mice. Mice of neurogenesis impairment with K252a or temozolomide (TMZ) administration for 4 weeks showed higher stress vulnerability than control mice to the sCMS paradigm (Fig. 6D). The experiments either blocking BDNF signaling with K252a or suppressing neurogenesis with TMZ abolished similarly the antidepressant effects of IL4-driven microglia based on the SPT and FST (Fig. 6E and fig. S9). These results suggested that IL4-driven Arg1^{+} microglia enhance hippocampal neurogenesis and stress resistance of CMS-exposed mice via a BDNF-dependent pathway.

DISCUSSION

Microglia are endowed with phenotypic plasticity, which can be stimulated by different cytokines to regulate physiological responses and behavioral outcomes during stress (*22*). In particular, IL4 induces Arg1^{+} microglial phenotype and promotes neural repair (*17*). The present study provides, to the best of our knowledge, the first direct evidence that IL4-driven microglia are essential for hippocampal neurogenesis and that they can mediate the resilience to chronic stress. The promotion of neurogenesis by IL4-driven Arg1^{+} microglia was associated with up-regulation of BDNF in the hippocampus. Thus, our study demonstrates that IL4-driven Arg1^{+} microglia ameliorate chronic stress–induced depressive-like behaviors in mice through BDNF-dependent neurogenesis.

The underlying immune environment alters the interaction between stress and inflammatory processes, thus contributing to the risk of depressive symptoms (*23*). In our study, we found that the levels of IL4 were decreased in the hippocampus of HS mice but increased in LS mice. Vulnerability to chronic stress is associated with dysregulation of pro- and anti-inflammatory cytokines, in particular an ineffective IL4 pathway (*19*). It was previously described that neuron and glia produced cytokines in CNS in animals exposed to stress, although the entry of peripheral cytokines into the parenchyma could not be completely ruled out, due to the blood-brain barrier impairment (*24*, *25*). In the present study, we demonstrated that neurons abundantly expressed IL4 with RNAscope-fluorescent probes in LS mice. The neuron-producing IL4 corresponded to microglia-harbored IL4R, representing a cross-talk mechanism of neuron-microglia in stress response. The reduction of IL4 levels can render individuals more vulnerable to stress and more likely to engage in depressive-like behaviors. IL4 deficiency increases stress vulnerability and risk of mood disorders (*18*). Our results, together
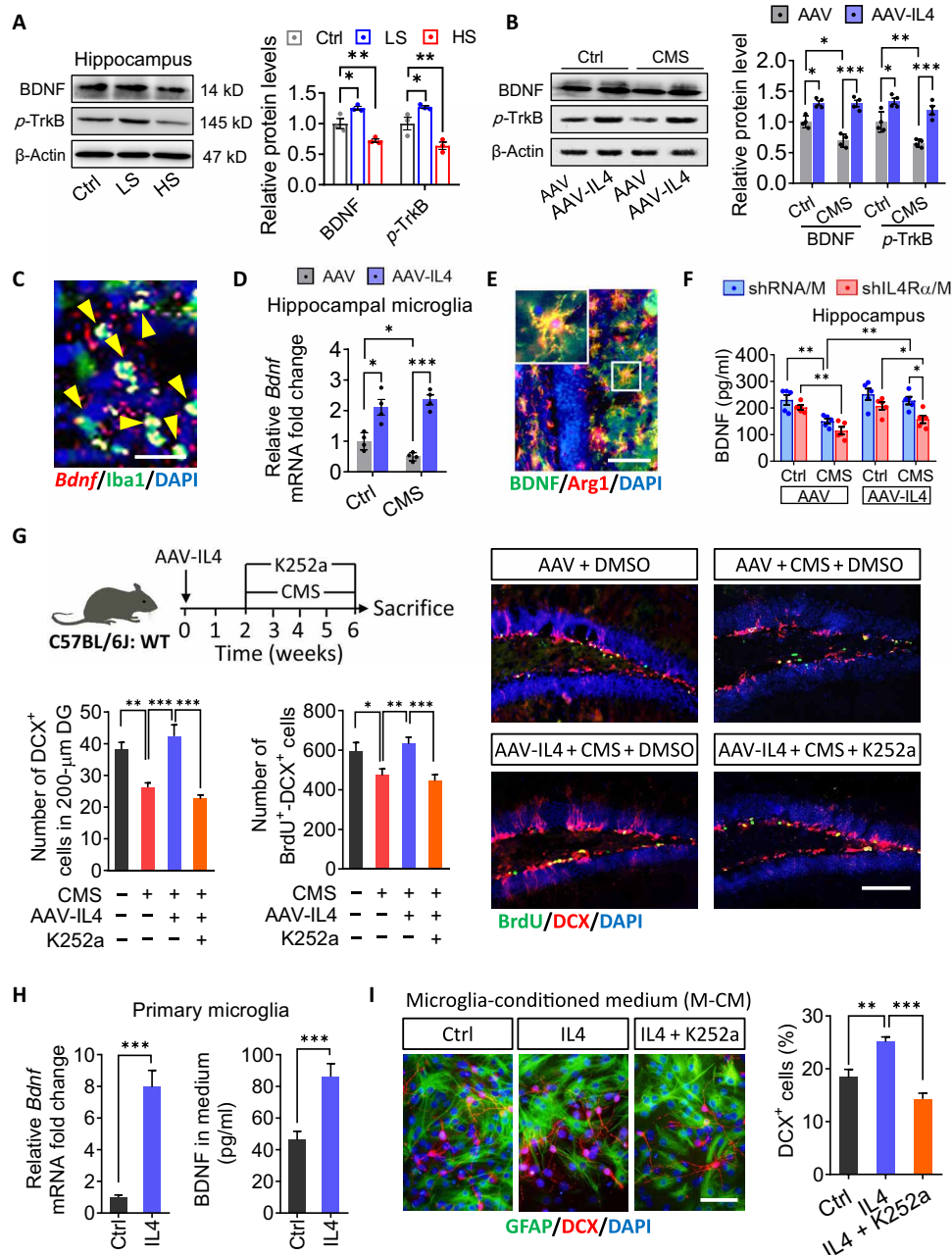
Fig. 5. IL4-driven microglia modulate adult hippocampal neurogenesis in a BDNF-dependent manner. (**A**) Western blotting shows the levels of BDNF and TrkB in the hippocampus of LS and HS mice. BDNF and TrkB are normalized to β-actin ($n = 3$). (**B**) Western blotting shows the levels of BDNF and TrkB in the hippocampus of CMS and/or AAV-IL4–treated mice. BDNF and TrkB are normalized to β-actin ($n = 4$). (**C**) BDNF was detected in hippocampal microglia (Iba1^{+} cells) using *Bdnf*-RNAscope. (**D**) The mRNA expression of BDNF was observed in hippocampal microglia of AAV-IL4–treated mice ($n = 4$). (**E**) Double immunohistochemical staining of BDNF and Arg1 in the hippocampus of AAV-IL4 mice. Scale bar, 20 μm. (**F**) Effects of CMS, knockdown of microglial IL4Rα, and overexpression of IL4 on BDNF protein levels in the hippocampus ($n = 5$). (**G**) Effects of k252a treatment to block the BDNF/TrkB pathway on hippocampal neurogenesis in AAV-IL4 mice under CMS exposure. Representative fluorescence micrographs showing DCX expression and BrdU incorporation in the SGZ. Scale bar, 100 μm. Quantification of the number of DCX^{+} cells and total number of DCX[+]-BrdU^{+} cells in the neurogenic zones ($n = 5$). DMSO, dimethyl sulfoxide. (**H**) The expression and secretion of BDNF in primary microglia after IL4 treatment in vitro ($n = 6$). (**I**) Effects of anti-BDNF antibody or K252a on NSPC proliferation (BrdU^{+} cells) in the presence of the conditioned culture medium from IL4-treated microglia ($n = 5$). Scale bar, 20 μm. Data are presented as means ± SEM. *$P < 0.05$, **$P < 0.01$, ***$P < 0.005$, one-way ANOVA with Tukey test (A, G, and I), two-way ANOVA with Tukey test (B, D, and F), and two-tailed *t* test (H).

with evidence from the literature (*26, 27*), suggest that levels of hippocampal IL4 vary inversely with stress vulnerability.

Up-regulation of IL4 in the hippocampus protected mice from stress-induced depressive-like behaviors, consistent with the finding that IL4 overexpression has antidepressant effects (*19*). Our transcriptome analysis showed that CMS leads to decreased expression of genes related to immune regulation (Arg1, Irf7, Irf9, etc.) and increased expression of genes related to stress response (Myoc, Cdk5rap1, etc.).

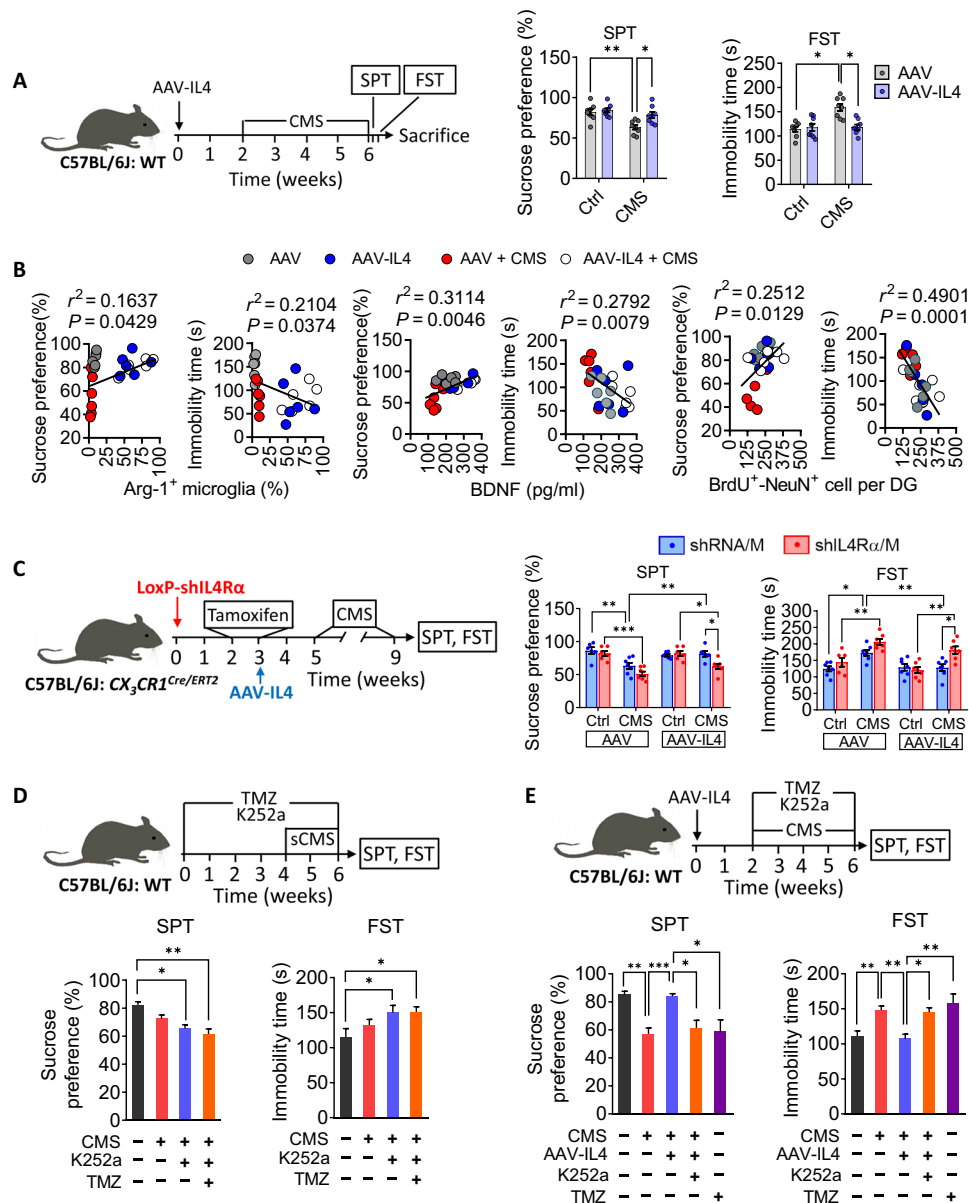**Fig. 6. IL4-driven Arg1+ microglia protected mice from stress-induced depressive-like behaviors.** (**A**) Effects of overexpression of IL4 in the hippocampus on stress-induced depressive-like behaviors. Mice were injected stereotactically with AAV-IL4 or AAV, allowed to recover for 2 weeks, and then subjected to a CMS protocol consisting of exposure to three random stressors daily for 4 weeks. The mice were assessed by SPT and FST (n = 8). (**B**) Correlations between sucrose preference and percentage of Arg1+ microglia in hippocampus, immobility time in FST and percentage of Arg1+ microglia in hippocampus, sucrose preference and concentration of BDNF in hippocampus, immobility time in FST and concentration of BDNF in hippocampus, sucrose preference and number of BrdU+-DCX+ cells in DG, and immobility time in FST and number of BrdU+-DCX+ cells in DG. Each circle represents one mouse (n = 6). (**C**) Effects of microglial IL4Rα down-regulation (before IL4 overexpression) on stress-induced depressive-like behaviors, as assessed by SPT and FST (n = 8 to 10). (**D**) Assessment of stress-induced depressive-like behaviors in WT mice when treated with K252a or TMZ with sCMS exposure (n = 8). (**E**) Assessment of stress-induced depressive-like behaviors in AAV-IL4 mice when treated with k252a or TMZ (n = 8 to 10). Data are presented as means ± SEM. *P < 0.05, **P < 0.01, ***P < 0.005, two-way ANOVA with Bonferroni test (A and C) and one-way ANOVA with Bonferroni test (D and E).

These results suggest that stress-induced depressive-like behaviors are associated with neuroimmune regulation (28). Overexpression of IL4 in the hippocampus of CMS-exposed mice leads to increased expression of a large number of immune-related genes, suggesting that increased immune regulation in the hippocampus can increase stress resistance. Among them, Arg1 is the most significantly up-regulated gene, and it is colocalized with microglia. Hence, overexpression of IL4 could significantly increase the number of Arg1+ microglia in hippocampus. Increased number of Arg1+ microglia was also found in hippocampus of LS mice, corresponding to up-regulated IL4 and enhanced IL4 receptor signaling. Meanwhile, the number of Arg1+ microglia decreased in hippocampus of HS mice. These results suggested that hippocampal Arg1+ microglia modulated by IL4 signaling is implicated in animal stress resistance. It is worth mentioning that although AAV vector–mediated in vivo reprogramming of microglial phenotypes is widely used in adult

mice (29), the local tissue damage and microglial activation resulted from AAV infection is an aspect to be taken into consideration.

IL4-induced Arg1$^+$ microglia can be thought of a special phenotype of beneficial microglia (21, 30). These cells regulate inflammatory processes in the brain and enhance neurite growth, thereby exhibiting neuroprotective effects (20, 31). In our study, CMS-exposed mice with a lower level of hippocampal IL4 showed fewer Arg1$^+$ microglia and higher levels of proinflammatory mediators such as IL1β, tumor necrosis factor–α, interferon-γ, and iNOS. In contrast, overexpression of IL4 in the hippocampus significantly increased Arg1$^+$ microglia and suppressed levels of proinflammatory mediators. These findings suggest that IL4-driven Arg1$^+$ microglia reduce inflammation in the hippocampus of CMS-exposed mice by reducing the synthesis and secretion of proinflammatory mediators. Further, the results from flow cytometry analysis of single-cell suspensions from the whole hippocampus showed that microglia, in the form of CD45^{int}-CD11b$^+$ cells, increased significantly in AAV-IL4 mice. These data indicate that IL4-induced Arg1$^+$ microglia are characterized by high proliferative activity. Furthermore, CD86$^+$-CD206$^+$ microglia were significantly increased in the hippocampus of AAV-IL4 mice, suggesting that IL4 mediates neuroprotective effects in the CNS mainly by driving the phenotypic shift of microglia. Significantly, knockdown of microglial IL4Rα decreased the number of Arg1$^+$ microglia and abrogated the antidepressant effects of IL4 overexpression, suggesting that IL4-driven Arg1$^+$ microglia play a key role in protecting from CMS-induced depressive-like behaviors. In the mice of microglial IL4Rα knockdown, the depressive-like behaviors responded to subliminal stress, accompanying with reduced numbers of Arg1$^+$ microglia and exaggerated inflammatory processes. The phenomena were similar to those shown in HS mice. These results suggested that decreasing the Arg1$^+$ microglia in the hippocampus by knocking down the microglial IL4R enhanced stress vulnerability.

Microglia constitute a prominent cell population within the hippocampal neurogenic niche (8). Our results confirmed that CMS resulted in proinflammatory activation of microglia and inhibition of hippocampal neurogenesis. The transcriptome sequencing showed that overexpression of IL4 in CMS-exposed mice induced microglial proneurogenic phenotype and mitigated stress-induced neurogenesis impairment. Knockdown of microglial IL4Rα of mice decreased the number of Arg1$^+$ microglia, blocked IL4-rescued hippocampal neurogenesis and stress resistance in CMS-treated mice. The data from in vitro assays showed that microglia isolated from hippocampus of CMS-exposed mice suppressed NSPC proliferation and neurogenesis. Meanwhile, microglia isolated from hippocampus of AAV-IL4 mice were sufficient to enhance NSPC proliferation and neuronal differentiation. Considering that microglia isolated from the brain may not maintain the same functions as microglia in vivo (32), we used the M-CM from IL4-stimulated primary microglia to culture NSPCs. Although the differences of biologies between the cultured microglia in vitro and the hippocampal microglia encumber interpretation of these results, the RNAscope data confirmed that overexpression of IL4 in vivo induced BDNF-producing Arg1$^+$ microglia. The result confirmed that IL4-driven Arg1$^+$ primary microglia could promote the proliferation and differentiation of NSPCs. These effects were not observed when IL4 was added directly to NSPCs, which indicated that IL4 rescued the impairment of adult neurogenesis in CMS-exposed mice in a microglia-dependent manner (33–35). Inhibition of neurogenesis in vivo with TMZ increased

stress vulnerability to sCMS and abolished the antidepressant effects of IL4-activated microglia in CMS-treated mice. Adult hippocampal neurogenesis appears to occur in humans as well as in rodents, although this idea is still controversial (36, 37). The relatively small number of new neurons in adult brains of humans and rodents is strongly linked to the pathogenesis and remission of neuropsychiatric disorders (38). These findings suggest that microglia-mediated proneurogenesis underlies resistance to stress-induced depression.

IL4 drove microglia to adopt a phenotype of alternative activation in CMS-exposed mice, associated with higher levels of BDNF release. Although BDNF/TrkB signaling was reduced in the hippocampus of CMS-exposed mice, the transcriptome sequencing with GO enrichment analysis showed that BDNF signaling–related genes were enriched to a high degree in AAV-IL4 mice. Furthermore, we found that abundant BDNF is produced by Arg1$^+$ microglia. Knockdown of microglial IL4Rα decreased the BDNF levels in the hippocampus of AAV-IL4 mice. Blocking of BDNF/TrkB signaling with k252a blocked IL4-rescued hippocampal neurogenesis and abolished stress resistance in AAV-IL4 mice. In addition, blocking BDNF/TrkB signaling in vitro also eliminated microglia-mediated neurogenesis. These findings suggest that the proneurogenesis effects of IL4-driven Arg1$^+$ microglia depend on BDNF/TrkB signaling. Because microglia are myeloid in origin, different from nerve cells, they are believed to influence neuronal behavior through noncontact-dependent pathways (6). BDNF is an important regulator of hippocampal neurogenesis and is necessary for neurobehavioral plasticity (11, 39). Our results suggest that the proneurogenesis effects and therefore the resiliency to stress of IL4-driven Arg1$^+$ microglia depend on BDNF/TrkB signaling. To this point, further studies with microglia-specific BDNF depletion are needed to determine the microglial BDNF-mediated neurogenic effects.

The present study identified critical roles of Arg1$^+$ microglia-mediated proneurogenesis in the modulation of vulnerability or resistance of mice to stress. Reprogramming microglia with IL4 can rescue hippocampal neurogenesis in stressed mice by increasing BDNF signaling. These findings indicate that regulation of microglial function is a potential therapeutic strategy for the treatment of mood disorders.

MATERIALS AND METHODS
Animals
$CX_3CR1^{Cre/ERT2}$ mice on a C57BL/6J background were purchased from the Jackson laboratory. Wild-type (WT) C57BL/6J mice were purchased from the Laboratory Animal Center of Sichuan Academy of Medical Sciences (Chengdu, China). All mice were housed under standard conditions with free access to food and water. All animal experiments were approved by the Ethics Committee of the University of Electronic Science and Technology of China and carried out in strict accordance with the U.S. National Institutes of Health *Guide for the Care and Use of Laboratory Animals* (eighth edition, revised 2010).

Chronic mild stress
Male mice aged 8 to 10 weeks at the start of experiments were caged individually and subjected to a CMS protocol (28). To establish an animal model of depression, the CMS paradigm was conducted over a 4-week period and consisted of daily exposure to three stressors in

random order. To screen the vulnerable animals, the CMS paradigm was conducted over a 3-week period. To perform sCMS, the CMS paradigm was conducted over a 2-week period. These stressors included empty water bottles (12 hours), food deprivation (12 hours), tail clipping (10 min), restraint (2 hours), lights-off for 3 hours during the daylight phase, cage shaking (1 hour), cage tilting (45°, 24 hours), reversal of the light-dark cycle (24 hours), strobe lighting (12 hours), damp bedding (24 hours), and a soiled cage (24 hours).

Animal screening

Mice were subjected to CMS for 3 weeks and then subdivided as described (40) into groups of HS or LS animals. The mice were considered LS if their immobility time in the FST and TST and their sucrose intake (see below) were within 1 SD of the mean values for control mice. If these values fell outside this threshold, then animals were considered HS.

Expression systems and stereotactic injection

rAAV 2/9 was produced by transfecting 293T cells with three plasmids: an AAV vector expressing both IL4 and enhanced green fluorescent protein (EGFP), IL4 alone, or EGFP alone; an AAV helper plasmid (pAAV Helper); and an AAV Rep/Cap expression plasmid. At 72 hours after transfection, cells were collected and lysed using a freeze-thaw procedure. AAV-IL4 or AAV was diluted to 1×10^{10} transforming units (TU)/ml and injected (0.5 μl) bilaterally in the hippocampus (Bregma, 2.3 mm; Lateral, 1.8 mm; Vertical, 2.0 mm).

To down-regulate expression of the IL4Rα in hippocampal microglia, a lentivirus encoding an shRNA against the receptor was constructed as described (41). The lentivirus contained the cassette u6-LoxP-stop-LoxP-shRNA-IL4Rα. To construct shRNA-IL4Rα, oligonucleotides containing antisense sequences were connected with a hairpin loop, followed by a poly termination signal. The sequences targeting IL4Rα (GenBank accession: NM_001008700, ID: 16190) in this experiment were 5′-GCG CTG TAT GGA GCT GTT TGA-3′ and 5′-TCA AAC AGC TCC ATA CAG CGC-3′.

For in vivo viral injections, viral vectors were bilaterally targeted to the hippocampus (Bregma, 2.3 mm; L, 1.8 mm; V, 2.0 mm). Animals received intracranial viral injections while under 10% pentobarbital anesthesia using a Kopf stereotactic apparatus. Mice were secured using ear bars and a head holder. A Micro-1 microsyringe pump controller (RWD Life Science, Shenzhen, China) was used to inject viral vectors. A 33-GA needle was lowered 2 mm over 5 min resulting in delivery of 0.25-μl viral vectors (2.5×10^9 TU) into each hippocampus. After injection, the syringe was held in place for 5 min to avoid backflow. Animals were sutured and placed on a heating pad for recovery. Mouse behavior was analyzed at 2 weeks after these injections (see below). Tamoxifen (Sigma-Aldrich, Missouri, USA) was dissolved in warm sunflower seed oil at a concentration of 40 mg/ml and injected intraperitoneally at 100 mg/kg for 7 days to induce Cre recombinase expression.

Pharmacological intervention

For a total of 4 weeks, mice in both intervention groups, the TMZ or K252a (a pharmacological inhibitor of TrkB), and the control group received daily intraperitoneal injections. Among them, the mice in the TMZ group were injected with TMZ (Sigma-Aldrich, Missouri, USA) at a concentration of 25 mg/kg (2.5 mg/ml in 0.9% NaCl containing 5% dimethyl sulfoxide); those in K252a group were injected

with K252a (Cell Signaling Technology, Boston, USA) at a concentration of 25 μg/kg (2.5 μg/ml in NaCl containing 5% dimethyl sulfoxide); the controls were injected with the vehicle everyday.

Behavioral analyses

Sucrose preference test

The sucrose preference test was performed as described (28). Mice were individually housed, deprived of food and water for 12 hours, and then given access to 1% sucrose solution (A) and water (B) for 2 hours. The bottle positions were switched daily to avoid a side bias. The sucrose preference was calculated each week for each mouse using the formula $100 \times [\text{VolA}/(\text{VolA} + \text{VolB})]$. The sucrose consumption was normalized to body weight for each mouse.

Forced swim test

Each mouse was placed for 15 min in a cylinder containing 15 cm of water. After 24 hours, the animals were placed again in the cylinder for 6 min. The duration of immobility (including staying afloat and movements to stay afloat) was measured using FST100 software (Taimeng Tech, Chengdu, China) during the last 4 min of swimming time.

Tail suspension test

The TST was performed as described (28). Mice were elevated by securing the tail 30 cm above the ground with adhesive plaster. Mice were isolated from one another using a black cardboard. Mice were recorded for 6 min, and time spent immobile during that period was determined by observers blind to mouse group allocations.

Gene expression analysis

Total RNA was isolated from mouse hippocampus or hippocampal microglia (see below) using Isol-RNA Lysis Reagent (5 Prime). Quantitative real-time PCR was performed, and gene expression was quantified using the $-\Delta\Delta C_t$ method. Primer sequences are listed in table S1.

Enzyme-linked immunosorbent assay

Hippocampal sections of mice were sonicated in radioimmuno-precipitation assay (RIPA) buffer containing protease inhibitors. Cytokine concentrations were quantified using enzyme-linked immunosorbent assay kits (QuantiCyto, Wuhan, China) according to the manufacturer's protocol. Detection limits were 8 pg/ml for IL4 and Arg1 and 4 pg/ml for iNOS and BDNF.

Western blotting

Hippocampal tissue or isolated hippocampal microglia (see below) were sonicated in RIPA buffer containing protease inhibitors. Hippocampal microglia from four mice were mixed into a sample, each sample in triplicate. Protein samples were run on 12% tris-glycine SDS–polyacrylamide gel electrophoresis gels, transferred to polyvinylidene difluoride membrane (0.2 or 0.45 μm), and blotted with antibodies against IL4 (1:1000), IL4Rα (1:1000), STAT6 (1:800), pSTAT6 (1:800), Arg1 (1:1000), iNOS (1:400), BDNF (1:800), TrkB (1:1000), p-TrkB (1:800), and β-actin (1:20,000). Primary antibody was incubated overnight at 4°C, and secondary antibodies (1:10,000; Abcam) were incubated for 2 hours at room temperature. Signals were developed using the ECL-Plus kit (Millipore, USA). Densitometry was performed to quantify signal intensity using ImageJ software (version 1.45 J; National Institutes of Health, Bethesda, MD, USA).

BrdU incorporation

To determine cell proliferation in the brain, mice received two intraperitoneal injections of BrdU (50 mg/kg) 8 hours apart. To examine progenitor proliferation, mice were euthanized 24 hours

after the second injection; to examine progenitor differentiation, mice were euthanized 1 week after BrdU injection. For examination of neuronal survival in the granular layer, animals were injected with a double dose of BrdU and euthanized 4 weeks after injection.

Tissue preparation and immunohistochemistry
Tissue preparation and staining were performed as described (28) using the antibodies listed in table S2.

Isolation of microglia from hippocampus
Hippocampus was isolated from the brain and homogenized into single-cell suspensions, from which microglia were isolated on a Percoll density gradient as described (42). Briefly, the hippocampus was homogenized, and cell pellets were resuspended in 70% isotonic Percoll. A discontinuous Percoll density gradient (70, 50, 35, and 0%) was layered and centrifuged for 20 min at 2000g. Enriched microglia were collected from the interphase between 70 and 50% Percoll. Of the cells recovered from this Percoll interphase, approximately 90% of the cells were $CD45^{int}$-$CD11b^{+}$ microglia.

Flow cytometry
Cells were assayed for surface antigens by flow cytometry as previously described (43). These microglia were labeled with fluorescein isothiocyanate anti-mouse CD45 (2 μg/ml; BioLegend, California, USA), APC (Allophycocyanin) anti-mouse CD11b (5 μg/ml; BioLegend, California, USA), APC/Cyanine7 anti-mouse CD86 (1 μg/ml; BioLegend, California, USA), and PerCP/Cyanine 5.5 CD206 (5 μg/ml; BioLegend, California, USA) antibodies for 30 min at room temperature. A four-laser Becton-Dickinson FACS Calibur (BD Biosciences, New Jersey, USA) was used to collect the data, and FlowJo software was used for analysis.

RNA sequencing
Total RNA was extracted from hippocampal tissue using TRIzol Reagent according to the manufacturer's instructions (Invitrogen, California, USA), and genomic DNA was removed using deoxyribonuclease I (TaKara, Tokyo, Japan). Then, RNA quality was determined by 2100 Bioanalyzer (Agilent, California, USA) and quantified using the ND-2000 (NanoDrop Technologies, Massachusetts, USA). Only high-quality RNA samples (OD260/280 = 1.8 to 2.2, OD260/230 ≥ 2.0, RIN (RNA integrity number) ≥ 6.5, 28S:18S ≥ 1.0, > 2 μg) were used to construct the sequencing library.

RNA purification, reverse transcription, library construction, and sequencing were performed according to the manufacturer's instructions (Illumina, California, USA). The RNA-seq transcriptome library was prepared following the TruSeqTM RNA sample preparation Kit from Illumina (California, USA) using 1 μg of total RNA. Briefly, mRNA was isolated according to poly A selection method by oligo (dT) beads and then fragmented using fragmentation buffer. Double-stranded cDNA was synthesized using a SuperScript double-stranded cDNA synthesis kit (Invitrogen, California, USA) with random hexamer primers (Illumina, California, USA). Then, the synthesized cDNA was subjected to end-repair, phosphorylation, and "A" base addition according to Illumina's library construction protocol. The size of libraries was selected for cDNA target fragments of 200 to 300 bp on 2% Low Range Ultra Agarose followed by PCR amplified using Phusion DNA polymerase (New England Biolabs, USA) for 15 cycles. After quantification by TBS380, paired-end RNA-seq library was sequenced on the Illumina NovaSeq 6000 (2 × 150 bp read length). All RNA-seq raw data were uploaded in Sequence Read Archive (SRA: PRJNA602066).

Analysis of RNA-seq data
RNA-seq data were initially filtered to obtain clean data, including removing reads with adaptors, reads with more than 10% unknown bases or low-quality reads (the percentage of low quality bases is more than 50% in the read). To identify DEGs between two different samples, the expression level of each transcript was calculated according to the fragments per kilobase of exon per million mapped reads method. The package software Empirical analysis of Digital Gene Expression in R (EdgeR) was used for differential expression analysis. In addition, functional enrichment analysis including GO and Kyoto Encyclopedia of Genes and Genomes (KEGG) was performed to identify which DEGs were significantly enriched in GO terms and metabolic pathways at Bonferroni-corrected P value ≤ 0.05 compared with the whole-transcriptome background. GO functional enrichment and KEGG pathway analysis were carried out by Goatools.

Cell culture and treatments
NSPCs and primary microglia were cultured as described (28). Microglia were treated with IL4 (20 ng/ml) for 24 hours to induce microglial activation (34). To assay the short-term effects of microglia on NSPCs, NSPCs were cocultured with microglia in transwell plates for 24 hours in experiments to examine proliferation or for 3 days in experiments to examine differentiation. To assay the long-term effects of microglia on NSPCs, NSPCs were cultured in M-CM for 24 hours in experiments to examine proliferation or for 7 days in experiments to examine differentiation. The BDNF pathway was blocked using anti-BDNF antibody (1 μg/ml; Abcam, Cambridge, UK) or BDNF receptor antagonist K252a (100 ng/ml).

RNAscope in situ hybridization
The experiment was to investigate the colocalization of IL4 and BDNF in different treatment groups. In situ hybridization was performed according to the protocol of the *Bdnf*-RNAscope Multiplex Fluorescent Probe Reagent Kit v2 and Mm-*Il4*-RNAscope 2.5 VS Fluorescent Probe Reagent Kit (Advanced Cell Diagnostics, California, USA). To detect source of IL4 and BDNF in CNS, Iba1 antibody (Gene Tex, Texas, USA), glial fibrillary acidic protein (GFAP) antibody (Cell Signaling Technology, Boston, USA), and NeuN antibody (Cell Signaling Technology, Boston, USA) were labeled for microglia, astrocyte, and neuron, respectively, by immunofluorescence.

Imaging and statistical analyses
Images were acquired using a Zeiss AxioImager Z1, and cells were counted manually. Areas of Iba1 staining and relative fluorescence intensity were analyzed using ImageJ software. Branches of microglia were measured using Image-Pro Plus 6.0 (Media Cybernetics, USA). To quantify total cell populations in the hippocampus (microglia, $BrdU^{+}$ cells, $BrdU^{+}$-DCX^{+} cells, and $BrdU^{+}$-$NeuN^{+}$ cells), every sixth section (25 μm thick) of the brain containing hippocampus was selected and immunostained. Total numbers of positive cells in all slices per animal were multiplied by six to estimate the number of cells per hippocampus. For measurement of the volume of hippocampus, DG and granule cell layer (GCL), every sixth section (25 μm thick) of the brain containing hippocampus was selected and labeled with DAPI (4′,6-diamidino-2-phenylindole). Total area of hippocampus, DG, or GCL in all slices per animal was multiplied by six to estimate the volume of hippocampus, DG, and GCL.

All quantitative results were expressed as means ± SEM. Data were plotted and analyzed statistically using GraphPad Prism 7.0. Data distribution was tested for normality with the Shapiro-Wilk test. Potential differences between the mean values were evaluated using one- or two-way analysis of variance (ANOVA), followed by the Bonferroni's (behavioral analysis) or

Tukey's (multiple comparison in addition to behavioral analysis) method for post hoc comparisons assuming equal variances. Two-tailed t tests were used to compare the differences between two groups, unless otherwise specified. Asterisks were used to indicate significance: $*P < 0.05$, $**P < 0.01$, and $***P < 0.001$. Values > 0.05 were considered not significant (ns).

SUPPLEMENTARY MATERIALS

Supplementary material for this article is available at http://advances.sciencemag.org/cgi/content/full/7/12/eabb9888/DC1

View/request a protocol for this paper from *Bio-protocol*.

REFERENCES AND NOTES

1. N. D. Hanson, M. J. Owens, C. B. Nemeroff, Depression, antidepressants, and neurogenesis: A critical reappraisal. *Neuropsychopharmacology* **36**, 2589–2602 (2011).
2. C. Anacker, V. M. Luna, G. S. Stevens, A. Millette, R. Shores, J. C. Jimenez, B. Chen, R. Hen, Hippocampal neurogenesis confers stress resilience by inhibiting the ventral dentate gyrus. *Nature* **559**, 98–102 (2018).
3. D. B. L. Teh, T. Ishizuka, H. Yawo, Regulation of later neurogenic stages of adult-derived neural stem/progenitor cells by L-type Ca^{2+} channels. *Dev. Growth Differ.* **56**, 583–594 (2014).
4. A. J. Eisch, D. Petrik, Depression and hippocampal neurogenesis: A road to remission? *Science* **338**, 72–75 (2012).
5. P. Rotheneichner, S. Lange, A. O'Sullivan, J. Marschallinger, P. Zaunmair, C. Geretsegger, L. Aigner, S. Couillard-Despres, Hippocampal neurogenesis and antidepressive therapy: Shocking relations. *Neural Plast.* **2014**, 723915 (2014).
6. R. Yirmiya, N. Rimmerman, R. Reshef, Depression as a microglial disease. *Trends Neurosci.* **38**, 637–658 (2015).
7. T. Kreisel, M. G. Frank, T. Licht, R. Reshef, O. Ben-Menachem-Zidon, M. V. Baratta, S. F. Maier, R. Yirmiya, Dynamic microglial alterations underlie stress-induced depressive-like behavior and suppressed neurogenesis. *Mol. Psychiatry* **19**, 699–709 (2014).
8. K. Sato, Effects of microglia on neurogenesis. *Glia* **63**, 1394–1405 (2015).
9. A. S. Hill, A. Sahay, R. Hen, Increasing adult hippocampal neurogenesis is sufficient to reduce anxiety and depression-like behaviors. *Neuropsychopharmacology* **40**, 2368–2378 (2015).
10. A. M. Littlefield, S. E. Setti, C. Priester, R. A. Kohman, Voluntary exercise attenuates LPS-induced reductions in neurogenesis and increases microglia expression of a proneurogenic phenotype in aged mice. *J. Neuroinflammation* **12**, 138 (2015).
11. P. Z. Liu, R. Nusslock, Exercise-mediated neurogenesis in the hippocampus via BDNF. *Front. Neurosci.* **12**, 52 (2018).
12. C. N. Parkhurst, G. Yang, I. Ninan, J. N. Savas, J. R. Yates III, J. J. Lafaille, B. L. Hempstead, D. R. Littman, W.-B. Gan, Microglia promote learning-dependent synapse formation through brain-derived neurotrophic factor. *Cell* **155**, 1596–1609 (2013).
13. J. A. M. Coull, S. Beggs, D. Boudreau, D. Boivin, M. Tsuda, K. Inoue, C. Gravel, M. W. Salter, Y. De Koninck, BDNF from microglia causes the shift in neuronal anion gradient underlying neuropathic pain. *Nature* **438**, 1017–1021 (2005).
14. R. Reshef, T. Kreisel, D. Beroukhim Kay, R. Yirmiya, Microglia and their CX3CR1 signaling are involved in hippocampal- but not olfactory bulb-related memory and neurogenesis. *Brain Behav. Immun.* **41**, 239–250 (2014).
15. X. Tan, X. Du, Y. Jiang, B. O. A. Botchway, Z. Hu, M. Fang, Inhibition of autophagy in microglia alters depressive-like behavior via BDNF pathway in postpartum depression. *Front. Psych.* **9**, 434 (2018).
16. S. P. Gadani, J. C. Cronk, G. T. Norris, J. Kipnis, IL-4 in the brain: A cytokine to remember. *J. Immunol.* **189**, 4213–4219 (2012).
17. X. Zhao, H. Wang, G. Sun, J. Zhang, N. J. Edwards, J. Aronowski, Neuronal interleukin-4 as a modulator of microglial pathways and ischemic brain damage. *J. Neurosci.* **35**, 11281–11291 (2015).
18. N. Üçeyler, T. Topuzoğlu, P. Schießer, S. Hahnenkamp, C. Sommer, IL-4 deficiency is associated with mechanical hypersensitivity in mice. *PLOS ONE* **6**, e28205 (2011).
19. S. Wachholz, A. Knorr, L. Mengert, J. Plümper, R. Sommer, G. Juckel, A. Friebe, Interleukin-4 is a participant in the regulation of depressive-like behavior. *Behav. Brain Res.* **326**, 165–172 (2017).
20. J. D. Cherry, J. A. Olschowka, M. K. O'Banion, Arginase 1+ microglia reduce Aβ plaque deposition during IL-1β-dependent neuroinflammation. *J. Neuroinflammation* **12**, 203 (2015).
21. Y. Xia, Z. Zhang, W. Lin, J. Yan, C. Zhu, D. Yin, S. He, Y. Su, N. Xu, R. W. Caldwell, L. Yao, Y. Chen, Modulating microglia activation prevents maternal immune activation induced schizophrenia-relevant behavior phenotypes via arginase 1 in the dentate gyrus. *Neuropsychopharmacology* **45**, 1896–1908 (2020).
22. L. E. Santos, D. Beckman, S. T. Ferreira, Microglial dysfunction connects depression and Alzheimer's disease. *Brain Behav. Immun.* **55**, 151–165 (2016).
23. J. Pearson-Leary, D. Eacret, R. Chen, H. Takano, B. Nicholas, S. Bhatnagar, Inflammation and vascular remodeling in the ventral hippocampus contributes to vulnerability to stress. *Transl. Psychiatry* **7**, e1160 (2017).
24. A. Han, H. Yeo, M. J. Park, S. H. Kim, H. J. Choi, C.-W. Hong, M.-S. Kwon, IL-4/10 prevents stress vulnerability following imipramine discontinuation. *J. Neuroinflammation* **12**, 197 (2015).
25. J. D. Johnson, D. F. Barnard, A. C. Kulp, D. M. Mehta, Neuroendocrine regulation of brain cytokines after psychological stress. *J. Endocrine Soc.* **3**, 1302–1320 (2019).
26. C. Ménard, M. L. Pfau, G. E. Hodes, S. J. Russo, Immune and neuroendocrine mechanisms of stress vulnerability and resilience. *Neuropsychopharmacology* **42**, 62–80 (2017).
27. H.-j. Lee, H.-J. Park, A. Starkweather, K. An, I. Shim, Decreased interleukin-4 release from the neurons of the locus coeruleus in response to immobilization stress. 2016, 3501905 (2016).
28. J. Zhang, X. Xie, M. Tang, J. Zhang, B. Zhang, Q. Zhao, Y. Han, W. Yan, C. Peng, Z. You, Salvianolic acid B promotes microglial M2-polarization and rescues neurogenesis in stress-exposed mice. *Brain Behav. Immun.* **66**, 111–124 (2017).
29. M. E. Maes, G. Colombo, R. Schulz, S. Siegert, Targeting microglia with lentivirus and AAV: Recent advances and remaining challenges. *Neurosci. Lett.* **707**, 134310 (2019).
30. B. Ma'arif, M. Agil, H. Laswati, The enhancement of Arg1 and activated ERβ expression in microglia HMC3 by induction of 96% ethanol extract of *Marsilea crenata* Presl. leaves. *J. Basic Clin. Physiol. Pharmacol.* **30**, 10.1515/jbcpp-2019-0284, (2019).
31. C. M. Toedebusch, J. C. Snyder, M. R. Jones, V. B. Garcia, G. C. Johnson, E. L. Villalón, J. R. Coates, M. L. Garcia, Arginase-1 expressing microglia in close proximity to motor neurons were increased early in disease progression in canine degenerative myelopathy, a model of amyotrophic lateral sclerosis. *Mol. Cell. Neurosci.* **88**, 148–157 (2018).
32. O. Butovsky, M. P. Jedrychowski, C. S. Moore, R. Cialic, A. J. Lanser, G. Gabriely, T. Koeglsperger, B. Dake, P. M. Wu, C. E. Doykan, Z. Fanek, L. Liu, Z. Chen, J. D. Rothstein, R. M. Ransohoff, S. P. Gygi, J. P. Antel, H. L. Weiner, Identification of a unique TGF-β–dependent molecular and functional signature in microglia. *Nat. Neurosci.* **17**, 131–143 (2014).
33. A. S. Paintlia, M. K. Paintlia, I. Singh, A. K. Singh, IL-4-induced peroxisome proliferator-activated receptor γ activation inhibits NF-κB trans activation in central nervous system (CNS) glial cells and protects oligodendrocyte progenitors under neuroinflammatory disease conditions: Implication for CNS-demyelinating diseases. *J. Immunol.* **176**, 4385–4398 (2006).
34. O. Butovsky, Y. Ziv, A. Schwartz, G. Landa, A. E. Talpalar, S. Pluchino, G. Martino, M. Schwartz, Microglia activated by IL-4 or IFN-γ differentially induce neurogenesis and oligodendrogenesis from adult stem/progenitor cells. *Mol. Cell. Neurosci.* **31**, 149–160 (2006).
35. P. Bhattarai, A. K. Thomas, M. I. Cosacak, C. Papadimitriou, V. Mashkaryan, C. Froc, S. Reinhardt, T. Kurth, A. Dahl, Y. Zhang, C. Kizil, IL4/STAT6 signaling activates neural stem cell proliferation and neurogenesis upon Amyloid-β42 aggregation in adult zebrafish brain. *Cell Rep.* **17**, 941–948 (2016).
36. S. F. Sorrells, M. F. Paredes, A. Cebrian-Silla, K. Sandoval, D. Qi, K. W. Kelley, D. James, S. Mayer, J. Chang, K. I. Auguste, E. F. Chang, A. J. Gutierrez, A. R. Kriegstein, G. W. Mathern, M. C. Oldham, E. J. Huang, J. M. Garcia-Verdugo, Z. Yang, A. Alvarez-Buylla, Human hippocampal neurogenesis drops sharply in children to undetectable levels in adults. *Nature* **555**, 377–381 (2018).
37. G. Kempermann, F. H. Gage, L. Aigner, H. Song, M. A. Curtis, S. Thuret, H. G. Kuhn, S. Jessberger, P. W. Frankland, H. A. Cameron, E. Gould, R. Hen, D. N. Abrous, N. Toni, A. F. Schinder, X. Zhao, P. J. Lucassen, J. Frisén, Human adult neurogenesis: Evidence and remaining questions. *Cell Stem Cell* **23**, 25–30 (2018).
38. J. S. Snyder, A. Soumier, M. Brewer, J. Pickel, H. A. Cameron, Adult hippocampal neurogenesis buffers stress responses and depressive behaviour. *Nature* **476**, 458–461 (2011).
39. G. Leal, C. R. Bramham, C. B. Duarte, BDNF and hippocampal synaptic plasticity. *Vitam. Horm.* **104**, 153–195 (2017).
40. C. Nasca, D. Bigio, D. Zelli, F. Nicoletti, B. S. McEwen, Mind the gap: Glucocorticoids modulate hippocampal glutamate tone underlying individual differences in stress susceptibility. *Mol. Psychiatry* **20**, 755–763 (2015).
41. B. Y. Nam, D. K. Kim, J. T. Park, H.-Y. Kang, J. Paeng, S. Kim, J. Park, J. E. Um, H. J. Oh, S. H. Han, T.-H. Yoo, S.-W. Kang, Double transduction of a Cre/LoxP lentiviral vector: A simple method to generate kidney cell-specific knockdown mice. *Am. J. Physiol. Renal Physiol.* **309**, F1060–F1069 (2015).
42. D. M. Norden, A. M. Fenn, A. Dugan, J. P. Godbout, TGFβ produced by IL-10 redirected astrocytes attenuates microglial activation. *Glia* **62**, 881–895 (2014).

43. A. M. Fenn, C. J. Henry, Y. Huang, A. Dugan, J. P. Godbout, Lipopolysaccharide-induced interleukin (IL)-4 receptor-α expression and corresponding sensitivity to the M2 promoting effects of IL-4 are impaired in microglia of aged mice. *Brain Behav. Immun.* **26**, 766–777 (2012).